2004年4月
東海大学　医の倫理委員会　承認
課題名：自家骨髄間葉系幹細胞を用いた
ヒト髄核細胞の活性化実験

2007年3月
東海大学　医の倫理委員会　承認
課題名：自家骨髄間葉系幹細胞により活性化された
椎間板髄核細胞を用いた椎間板再生研究

2007年4月
厚生労働省　ヒト幹細胞臨床研究に関する申請
臨床研究名：自家骨髄間葉系幹細胞により活性化された
椎間板髄核細胞を用いた椎間板再生研究

2007年11月26日
厚生労働省ヒト幹細胞臨床研究に関する審査委員会
研究実施計画を了承

Cell Processing Centerでの髄核細胞活性化の試行

細胞処理を行う技術職員の養成教育の修了

髄核細胞、骨髄細胞（MSC）受け入れ時試験、
培養5日目の髄核細胞、骨髄細胞（MSC）の工程管理試験、
培養8日目の最終製品（活性化髄核細胞）試験

細胞表面マーカーによる髄核細胞の解析の継続
得られた結果をもとに簡便なセミソリッド培養系における髄核細胞の機能的な細胞集団の同定法の開発
in vivoアッセイ系の開発

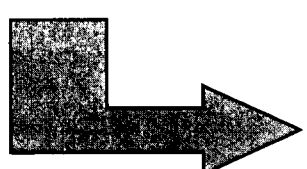

細胞指標の評価が可能となり、
臨床有効性との相関も解析可能

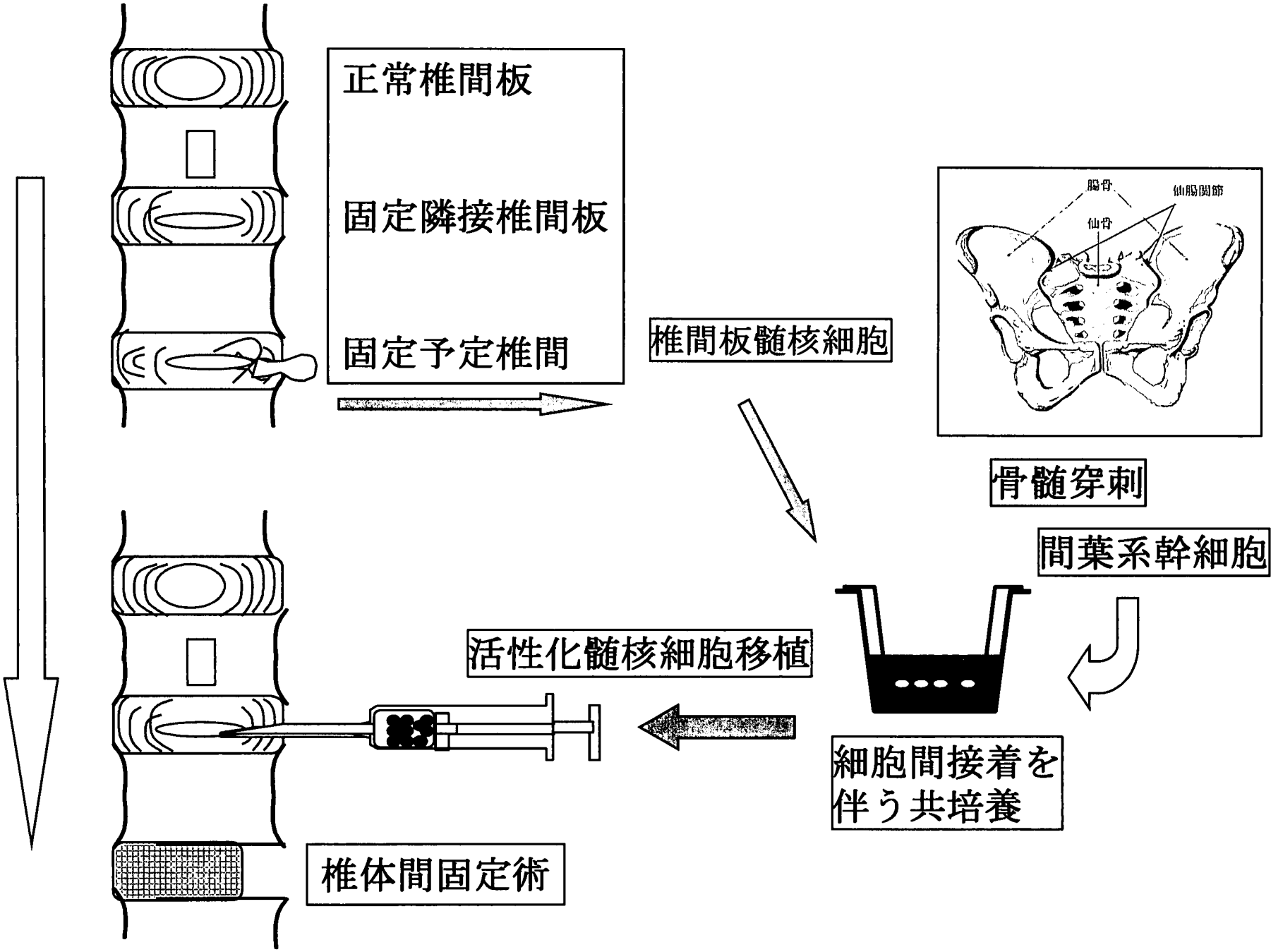
正常椎間板
固定隣接椎間板
固定予定椎間
椎間板髄核細胞
腸骨
仙腸関節
仙骨
骨髄穿刺
間葉系幹細胞
活性化髄核細胞移植
細胞間接着を
伴う共培養
椎体間固定術

JOURNAL OF BONE AND MINERAL RESEARCH
Volume 22, Number 12, 2007
Published online on August 13, 2007; doi: 10.1359/JBMR.070805

Expression of Acid-Sensing Ion Channel 3 (ASIC3) in Nucleus Pulposus Cells of the Intervertebral Disc Is Regulated by p75NTR and ERK Signaling

Yoshiyasu Uchiyama,[1,2] Chin-Chang Cheng,[1,3] Keith G Danielson,[1] Joji Mochida,[2] Todd J Albert,[1] Irving M Shapiro,[1] and Makarand V Risbud[1]

ABSTRACT: Although a recent study has shown that skeletal tissues express ASICs, their function is unknown. We show that intervertebral disc cells express ASIC3; moreover, expression is uniquely regulated and needed for survival in a low pH and hypoeromsotic medium. These findings suggest that ASIC3 may adapt disc cells to their hydrodynamically stressed microenvironment.

Introduction: The nucleus pulposus is an avascular, hydrated tissue that permits the intervertebral disc to resist compressive loads to the spine. Because the tissue is hyperosmotic and avascular, the pH of the nucleus pulposus is low. To determine the mechanisms by which the disc cells accommodate to the low pH and hypertonicity, the expression and regulation of the acid sensing ion channel (ASIC)3 was examined.
Materials and Methods: Expression of ASICs in cells of the intervertebral disc was analyzed. To study its regulation, we cloned the 2.8-kb rat ASIC3 promoter and performed luciferase reporter assays. The effect of pharmacological inhibition of ASICs on disc cell survival was studied by measuring MTT and caspase-3 activities.
Results: ASIC3 was expressed in discal tissues and cultured disc cells in vitro. Because studies of neuronal cells have shown that ASIC3 expression and promoter activity is induced by nerve growth factor (NGF), we examined the effect of NGF on nucleus pulposus cells. Surprisingly, ASIC3 promoter activity did not increase after NGF treatment. The absence of induction was linked to nonexpression of tropomyosin-related kinase A (TrkA), a high-affinity NGF receptor, although a modest expression of p75NTR was seen. When treated with p75NTR antibody or transfected with dominant negative-p75NTR plasmid, there was significant suppression of ASIC3 basal promoter activity. To further explore the downstream mechanism of control of ASIC3 basal promoter activity, we blocked p75NTR and measured phospho extracellular matrix regulated kinase (pERK) levels. We found that DN-p75NTR suppressed NGF mediated transient ERK activation. Moreover, inhibition of ERK activity by dominant negative-mitogen activated protein kinase kinase (DN-MEK) resulted in a dose-dependent suppression of ASIC3 basal promoter activity, whereas overexpression of constitutively active MEK1 caused an increase in ASIC3 promoter activity. Finally, to gain insight in the functional importance of ASIC3, we suppressed ASIC activity in nucleus pulposus cells. Noteworthy, under both hyperosmotic and acidic conditions, ASIC3 served to promote cell survival and lower the activity of the pro-apoptosis protein, caspase-3.
Conclusions: Results of this study indicate that NGF serves to maintain the basal expression of ASIC3 through p75NTR and ERK signaling in discal cells. We suggest that ASIC3 is needed for adaptation of the nucleus pulposus and annulus fibrosus cells to the acidic and hyperosmotic microenvironment of the intervertebral disc.
J Bone Miner Res 2007;22:1996–2006. Published online on August 13, 2007; doi: 10.1359/JBMR.070805

Key words: intervertebral disc, acid sensing ion channel, nucleus pulposus cells, p75NTR, extracellular matrix-regulated kinase, signaling

INTRODUCTION

THE INTERVERTEBRAL DISC is a specialized biomechanical structure that permits motion between vertebrae and absorbs mechanical loads. The disc is bounded by the endplate cartilages of adjacent vertebrae and a circumferential ligamentous structure, the annulus fibrosus. Contained within the disc are cells of the nucleus pulposus; there cells secrete matrix macromolecules, which by elevating the osmotic pressure, serve to accommodate applied mechanical forces. Whereas the nucleus pulposus cells are metabolically active, the vascular supply to the intervertebral disc is

The authors state that they have no conflicts of interest.

[1]Department of Orthopaedic Surgery, Thomas Jefferson University, Philadelphia, Pennsylvania, USA; [2]Department of Orthopaedic Surgery, Surgical Science, Tokai University School of Medicine, Bohseidai, Isehara, Kanagawa, Japan; [3]Department of Orthopaedic Surgery, Chang Gung Memorial Hospital, Chang Gung University, Taoyuan, Taiwan.

limited.[1] As a result, the nucleus pulposus cells generate almost all of their metabolic energy through the glycolytic pathway.[2,3] One consequences of the reliance on anaerobic metabolism is that the disc pH is low. How nucleus pulposus cells adapt to, and function in, an acidotic and hyperosmotic microenvironmental niche is not understood.

The mechanism by which tissues adapt to a low pH is tissue specific. In neural tissues, cells adjust to variations in the extracellular pH by regulating the activities of acid sensing ion channel (ASIC) proteins. These proteins are members of the amiloride-sensitive Na^+-channel/degenerin family. Four distinct genes encoding six ASIC isoforms have been identified.[4–9] These polypeptides form both homomeric and heteromeric functional membrane channels, most likely a tetramer, each with distinct electrophysiological characteristics.[10,11] Of these channel proteins, ASIC3s have been shown to be needed for maintenance of a number of physiological functions and are implicated in pain transduction associated with ischemic or inflamed tissue acidosis.[12–17] In general, these channel proteins respond to extracellular acidification by regulating transmembrane Na^+, K^+, or Ca^{2+} flux.

Because the nucleus pulposus can be regarded as a closed tissue compartment with a limited vascular supply, we explored the possibility that ASIC was expressed by intervertebral disc cells. Using cells of both the annulus fibrosus and nucleus pulposus, we show that there is expression of both ASIC3 and ASIC2b. Whereas in other tissues, ASIC3 expression is responsive to nerve growth factor (NGF), mediated by the high affinity receptor tropomyosin-related kinase A (TrkA), effects mediated through the low-affinity neurotrophin receptor, p75NTR, and mitogen activated protein kinase kinase (MEK)/extracellular matrix-regulated kinase (ERK) signaling were observed in cell from the intervertebral disc. Moreover, ASIC function is needed for survival at a low pH and at a high osmotic pressure. These new findings suggest that the activity of this channel protein may serve to adapt disc cells to their unique, hydrodynamically stressed microenvironment.

MATERIALS AND METHODS

Isolation of nucleus pulposus and annulus fibrosus cells

Rat nucleus pulposus and annulus fibrosus cells (male Wistar rats, 250 g) were isolated from the spine using a method reported earlier by Risbud et al.[3] and was approved by the Institutional Animal Care Committee of Thomas Jefferson University. Harvested cells were maintained in DMEM and 10% FBS. When confluent, the cells were lifted using a trypsin (0.25%) EDTA (1 mM) solution and subcultured in 10-cm dishes (2.0–3.0 × 10^5 cells/plate).

Immunohistological studies

Freshly isolated discs from adult rats were immediately fixed in 4% paraformaldehyde in PBS, whereas whole mouse embryos (E15.5) were perfusion fixed. Discs or embryos were embedded in paraffin. Transverse and coronal sections, 6–8 μm in thickness, were deparaffinized in xylene, rehydrated through graded ethanol, and stained with Alcian blue and with eosin and propidium iodide. For localizing ASIC3, sections were incubated with the anti-ASIC3 antibody (Neuromics) in 2% BSA in PBS at a dilution of 1:100 at 4°C overnight. After thoroughly washing the sections, the bound primary antibody was incubated with biotinylated universal secondary antibody at a dilution of 1:20 (Vector Laboratories) for 10 min at room temperature. Sections were incubated with a streptavidin/peroxidase complex for 5 min and washed with PBS, and color was developed using 3′-3-diaminobenzidine (Vecta Stain Universal Quick Kit; Vector Laboratories). Negative control for staining included use of isotype IgG (1:100). Some sections were counterstained with H&E and Alcian blue.

RT-PCR analysis

RNA was isolated from fresh tissue and cultured cells using Trizol reagent (Invitrogen) following the manufacturer's instructions. Briefly, 3 μg of total RNA was reverse transcribed into cDNA using Superscript II RT enzyme (Invitrogen) and oligo (dT) primers. PCR reactions were performed using cDNA samples (1 μl) with Superscript DNA polymerase (Invitrogen). Primers for rat genes were custom designed and synthesized by Integrated DNA Technologies (Coralville, IA, USA). The PCR product was run on a 1.2% agarose gel, and the amplicon was visualized on a Kodak 440 imaging station.

Immunofluorescence microscopy

Cells were plated in flat bottom 96-well plates (5000 cells/well) and maintained in complete medium for 24 h. After incubation, cells were fixed with 4% paraformaldehyde, permeabilized with 0.2% triton-X 100 in PBS for 10 min, blocked with PBS containing 5% FBS, and incubated with anti-ASIC3 antibody (1:200; Alpha Diagnostics) at 4°C overnight. As a negative control, cells were reacted with mouse isotype IgG under similar conditions. After washing, the cells were incubated with Alexa fluor-488 conjugated anti-mouse secondary antibody (Molecular Probes) at a dilution of 1:50 for 1 h at room temperature. Cells were washed and imaged using a laser scanning confocal microscope (Olympus Fluoview).

Nuclear and membrane protein extraction and Western blotting

Nuclear and membrane proteins from nucleus pulposus cells were isolated using CellLytic NuCLEAR extraction kit (Sigma-Aldrich) or Mem-PER eukaryotic membrane protein extraction reagent kit (Pierce), respectively, following manufacturer's instructions. To examine the glycosylation of ASIC3, total cell protein (50 μg) was denatured at 100°C in 0.5% SDS and 0.04 M DTT and treated with 2500 U of peptide N glycosidase F (PNGase F, New England Biolabs) in 0.05 M sodium phosphate buffer containing 1% NP-40 for 3 h. Protein extracts or total cell lysates were resolved on 10% SDS-polyacrylamide gels and electroblotted to PVDF membranes. The membranes were blocked with 5% nonfat dry milk in TBST (50 mM Tris, pH 7.6, 150 mM NaCl, 0.1% Tween 20) and incubated overnight at 4°C

in 3% nonfat dry milk in TBST with the anti-ASIC3 antibody from two different manufacturers (Alpha Diagnostics and Alamone Laboratories) at a dilution of 1:500, ASIC2b, 1:500 (Alpha Diagnostics), pERK and ERK, 1:1000 (Cell Signaling), p75NTR, 1:1000 and TrkA, 1:1000 (Abcam), pTrkA; and 1:1000 (Cell Signaling). Immunolabeling was detected using the ECL reagent (Amersham Biosciences).

Cloning of rat ASIC3 promoter

Genomic DNA was prepared from rat liver. PCR amplification of a 2925-bp fragment containing 2831 bp of the upstream promoter sequence linked to 94 bp of exon 1 (i.e., −2831 to +94) of the *ASIC3* gene (17, NCBI accession no. AF527125) was done using the following primers: forward 5′-GAGACGCGTCCTAGCCTTTGTGAGAGTC-TGCCCCA -3′, *Mlu*I site underlined; reverse 5′- GGT-CTCGAGAGTGAAGACCGAGTAGGGCAC -3′, *Xho*I site underlined) with the addition of GC buffer 1 and LA *Taq* polymerase (Takara Mirus Bio). Similarly, DNA sequences of 1571 bp (−1477 to +94) and 1065 bp (−971 to + 94) were amplified using one of the following forward primers: 5′-GAGACGCGTGGACTGATTGGTTGGTGG-GATTATGTCC-3′ or 5′-GAGACGCGTCCCCAAA-GCTCTCTCCTCATCTTCCT-3′, *Mlu*I sites underlined) and the same reverse primer noted above. The resulting DNA fragments were subcloned into pCR2.1 TA vector (Invitrogen), isolated by restriction digestion with *Mlu*I and *Xho*I, and ligated into the luciferase basic expression vector, pGL3 (Promega). The identity of each ASIC3 promoter sequence was confirmed by sequencing.

Plasmids

Plasmids were kindly provided by Dr Takahiro Suzuki, Tokyo Institute of Technology (TH-Luc reporter),[18] Dr Susan Meakin, Robarts Research Institute (pCMX-TrkA),[19] Dr Ramesh Ray, University of Tennessee, and Dr Natalie Ahn, University of Colorado (CA-MEK1, DN-MEK1).[20] Ecdysone inducible dominant negative p75NTR vector (DN-p75NTR) and ecdysone receptor expression plasmid pVgRxR were provided by Dr Daniel Djakiew, Georgetown University.[21] Gal4-ELK1-TAD and pFR-Luc reporter were from Stratagene. As an internal transfection control, vector pRL-TK (Promega) containing the *Renilla reniformis luciferase* gene was used.

Transfections and dual luciferase assay

Nucleus pulposus cells or PC12 cells (rat adrenal pheochromocytoma cells that respond to NGF) were transferred to 24-well plates at a density of 7.5×10^4 cells/well 1 day before transfection. LipofectAMINE 2000 (Invitrogen) was used as a transfection reagent. For each transfection, desired concentrations and combination of the plasmids were premixed with the transfection reagent. In some experiments, 24 h after transfection, cells were treated with NGF (100 ng/ml), anti-NGF (R&D Systems; 2 μg/ml), anti-TrkA (2 μg/ml), anti-p75NTR (2 μg/ml), or anti-NGF followed by NGF. When ecdysone-inducible DN-p75NTR plasmid was used, cells were treated with 1 μg pronesterin (a synthetic ecdysone analog; Invitrogen). The next day, the cells were harvested, and a Dual-Luciferase reporter assay system (Promega) was used for sequential measurements of firefly and Renilla luciferase activities. Quantification of luciferase activities and calculation of relative ratios were carried out using a liminometer (TD-20/20; Turner Designs).

Flow cytometry

Nucleus pulposus cells were analyzed for the expression of TrkA and p75NTR receptor. At 70% confluence, cells were detached from the tissue culture plates using a nonenzymatic digestion solution and washed twice with PBS. Cells were suspended in PBS supplemented with 5% FCS and treated with antibodies against TrkA and p75NTR (Abcam). After 1 h at 37°C, cells were washed twice with PBS and incubated with Alexa fluor 488 conjugated secondary antibody for 45 min in blocking buffer. After incubation, cells were washed thoroughly and subjected to flow cytometry using a Beckman Coulter XL setup equipped with a 488 argon ion laser and a four-color detector. Cells incubated with isotype antibody and a fluorescent secondary antibody were used as a negative control.

Measurement of cell survival

To measure cell viability, the MTT assay was carried out. Briefly, after pH or osmotic treatments, MTT diluted in PBS was added to the culture medium to a final concentration of 0.5 mg/ml. At the end of the incubation period (2–4 h at 37°C), the medium was removed, and the precipitated formazan crystals were solubilized in dimethyl sulfoxide. Product formation was measured by reading the absorbance at 560 nm in a microplate reader (Tecan; Spectra Fluor Plus).

Measurement of caspase-3 activation after ASIC inhibition

To determine if treatment of nucleus pulposus cells with the ASIC inhibitor amiloride in hypertonic media promoted cell death, we evaluated caspase-3 activation. Cells were cultured in isotonic (330 mosmol/kg) or hypertonic medium (450 mosmol/kg) and treated with amiloride (10–100 μM) for 24 h. After treatment, cleavage of the PhiPhi-Lux-G_1D_2 substrate (OncoImmune) was visualized following the manufacturer's protocol. Cells were imaged using a laser scanning confocal microscope (Olympus Fluoview). Quantitative image analysis was performed using 10 random fields of cells per experimental group. The 36-bit color images were recorded by confocal microscopy using the green channel. Image Proplus software (Media Cybernetics, Silver Spring, MD, USA) was used to calculate the threshold for all cells in the field. The mean density of PhiPhi Lux fluorescence was then plotted as a histogram.

Statistical analysis

All measurements were made from three independent experiments performed in triplicate. Data are presented as mean ± SD. Differences between groups were analyzed by Student's *t*-test at $p < 0.05$.

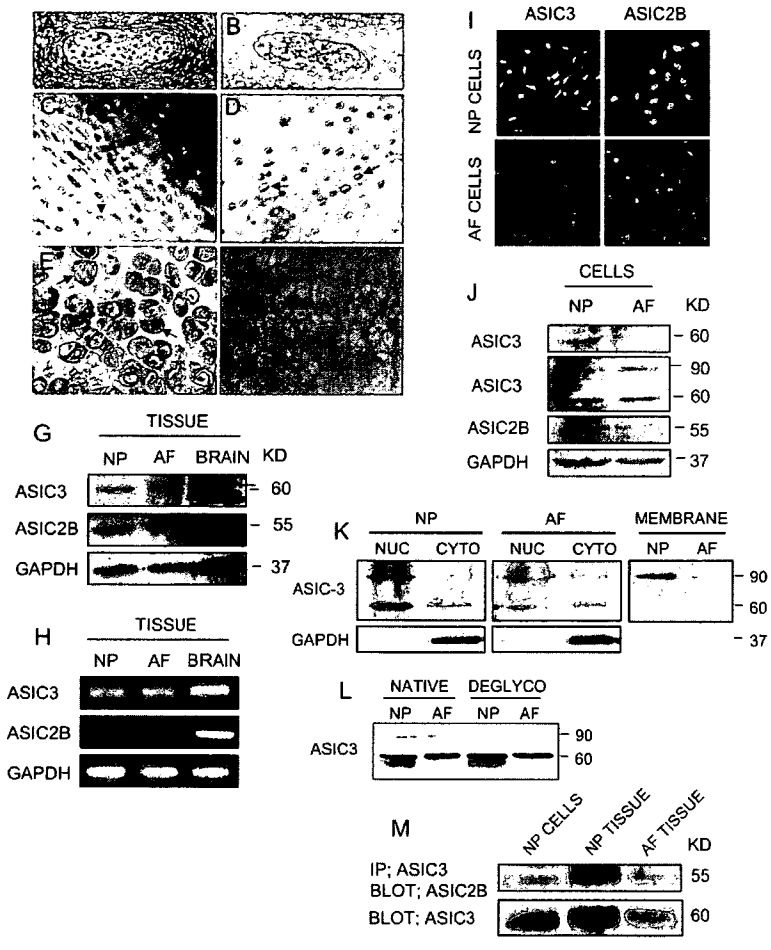

FIG. 1. Expression of ASICs in the rat intervertbral disc. Sagittal sections of the intervertebral disc of embryonic (A and B) and mature rat (C–F) spines. Sections were treated with anti-ASIC3 antibody (B, D, and F) or counterstained with Alcian blue, eosin, and hematoxylin (A, C, and E). Note that nucleus pulposus cells expressed ASIC3 protein (B; arrow; magnification, ×20). ASIC3 expression was also evident in mature rat disc in the inner annulus zone (D; arrows). These cells are surrounded by an Alcian blue–positive matrix and display a round morphology (C, arrows), whereas the outer annulus fibrosus cells are surrounded by eosinophilic collagen rich matrix (C, arrowhead). ASIC3 expression was not detectable in the endplate chondrocytes of mature rat discs (F), which exhibit a round hypertrophic phenotype (E, arrows; magnification, ×20). (G) Expression of ASIC3 and ASIC2b in the intervertebral disc. mRNA was extracted from the nucleus pulposus (NP), the annulus fibrosus (AF), and the brain of adult rats and subjected to RT-PCR analysis. There was expression of ASIC3 and ASIC2b in both the discal tissues. Brain maximally expressed both ASIC isoforms. (H) Western blot analysis of ASIC3 and ASIC2b from adult rat discal tissues. Both nucleus pulposus and annulus fibrosus expressed ASIC3 and ASIC2b. (I) Immunofluorescent detection of ASIC proteins in discal cells. Cells were treated with antibodies to ASIC3 and ASIC2b. Both nucleus pulposus and annulus fibrosus cells expressed ASIC3 and ASIC2b (magnification, ×20). (J) Western blot analysis of ASIC proteins in cell lysates of discal cells. Western blots were performed using antibodies to ASIC3 (two separate antibodies for ASIC3) and ASIC2b. Both ASIC3 antibodies recognized a band at 60 kDa and an additional high molecular weight band at 90 kDa. (K) ASIC3 protein expression in the nuclear, cytosolic, and membrane fractions of disc cells. Fractionated protein extracts of the nucleus pulposus and annulus fibrosus cells were probed by Western blot for the expression of ASIC3. Note the prominent expression of this protein in the all the fractions. (L) Effects of deglycoslylation on ASIC3 protein molecular weight. Cell lysates were deglycosylated using PNGase F for 3 h at 37°C and probed for expression of ASIC3. The molecular weight of ASIC3 peptides were unchanged by treatment with the enzyme. (M) Immunoprecipitation (IP) analysis of ASIC3 and ASIC2b in disc cells. IP analysis was performed on tissue and cell lysates using anti-ASIC3 antibody. Immune complexes were separated by SDS-PAGE and probed with anti-ASIC2b antibody. Note the presence of ASIC2b in the ASIC3 immunoprecipitate of both the nucleus pulposus and annulus fibrosus tissue and nucleus pulposus cells.

RESULTS

Sagittal sections of the embryonic and mature rat disc were stained with Alcian blue (Figs. 1A, 1C, and 1E) or with an antibody to ASIC3 (Figs. 1B, 1D, and 1F). ASIC3 is expressed by cells of both the nucleus pulposus (Fig. 1B) and the annulus fibrosus (Fig. 1D). In both cases, staining is localized to the plasma membrane. However, some staining is also seen in the cytosol of the nucleus pulposus cells of the embryonic discs (Fig. 1B). There is also a prominent expression of ASIC3 protein in the inner annulus fibrosus cells of the mature rat disc (Fig. 1D). In contrast to the

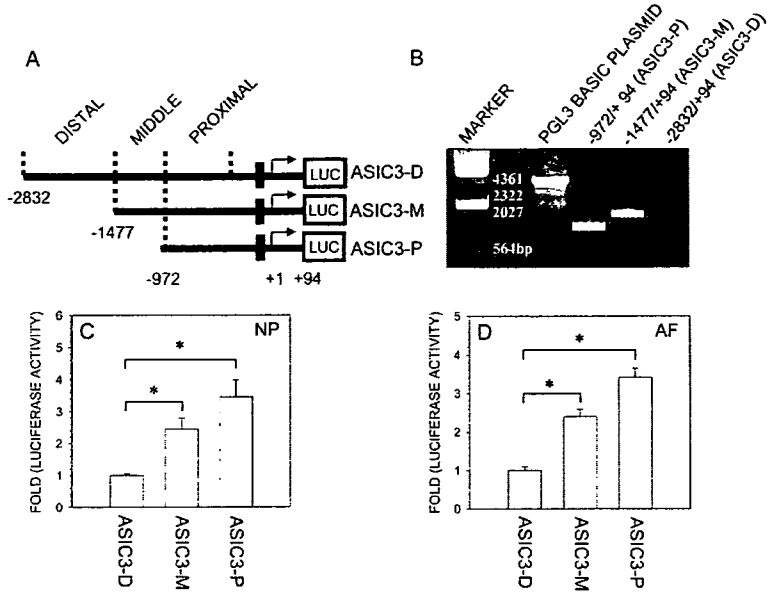

FIG. 2. Cloning of rat ASIC3 promoter and its activity in disc cells. (A) Cartoon showing map of successive PCR generated 5′ deletion constructs of the rat ASIC3 promoter. The ASIC3 promoter contains three distinct domains: proximal, middle, and a distal activating domain. The ASIC3-D construct consists of a 2925-bp fragment containing 2831 bp of the upstream ASIC3 promoter sequence linked to 94 bp of exon 1 (i.e., −2831 to +94), whereas ASIC3-M and ASIC3-P constructs contain a 1571- (−1477 to +94) and a 1065-bp (−971 to + 94) fragement, respectively. (B) Agarose gel electrophoresis showing PCR amplicons corresponding to different size fragments of the rat ASIC3 promoter. PCR was performed on rat liver genomic DNA using a set of nested forward primers containing a *MluI* site and a common reverse primer with a *XhoI* site. The resulting DNA fragments were ligated into *MluI* and *XhoI* digested luciferase basic expression vector, pGL3. (C and D) Basal activities of ASIC3 promoter constructs relative to full-length construct ASIC3-D in nucleus pulposus (C) and annulus fibrosus cells (D). Both the cell types showed maximal luciferase activity for the ASIC3-P construct, whereas the longest construct, ASIC3-D, containing all three promoter domains, showed minimal activity. Values shown are mean ± SE of three independent experiments. $*p < 0.05$.

other disc tissues, the endplate chondrocytes showed little or no ASIC3 staining (Fig. 1F). Western blot and RT-PCR analyses of the nucleus pulposus and annulus fibrosus tissue of the adult rat indicated that the cells express ASIC3 and ASIC2b proteins (Fig. 1G) and mRNA (Fig. 1H). Other ASIC isoforms could not be detected in the discal tissues. As expected, ASIC3 mRNA expression in the brain was the highest of all the tissues analyzed.

We studied the localization and expression levels of ASICs in cultured disc cells. Similar to the native tissues, cells of the nucleus pulposus and annulus fibrous expressed both ASIC3 and ASIC2b proteins (Figs. 1I and 1J). The ASIC isoforms were present in the plasma membrane and nuclear and cytosolic fractions. When probed with an antibody from Alpha Diagnostics, an ASIC3 band with a molecular weight of ~60 kDa was seen; a similar band, with a higher molecular weight (90 kDa), was evident when the blots were treated with an antibody from Alamone Laboratories (Fig. 1J). A second ASIC isoform was observed when the blots were probed with an antibody to ASIC2b. This protein has a molecular weight of 55 kDa and was present in extracts of the nucleus pulposus; in the annulus fibrosus, there was a low level of expression of ASIC2b. To further characterize their cellular localization, we probed the subcellular fractions for the presence of ASIC proteins. We found that the ASIC3 peptide with a molecular weight of 90 kDa was present in the nuclear, membrane and cytosolic fraction of the nucleus pulposus; this protein was weakly expressed by cells of the annulus fibrosus (Fig. 1K). To determine whether the different ASIC3 products expressed by disc cells were caused by variations in glycosylation status, we deglycosylated the protein using PNGase F. Western blot analysis, after deglycosylation, showed that there was no change in the molecular weight of the ASIC3 peptides before or after enzyme treatment. To further explore whether there was interaction between ASIC3 and ASIC2b, we immunoprecipitated ASIC3. Figure 1M shows that the immunoprecipitated protein complex from both nucleus cells and the native tissue contained ASIC2b. A second immunoprecipitation assay using an antibody to ASIC2b resulted in pulldown of ASIC3 (data not shown).

To determine whether there was a disc-specific regulation of ASIC3 expression, we cloned the 2.8-kb rat ASIC3 promoter into promoterless pGL3 basic luciferase plasmid and generated a series of 5′–3′ deletion fragments corresponding to different promoter domains (Figs. 2A and 2B). The activity of these promoter constructs was analyzed by transfection into nucleus pulposus and annulus fibrosus cells. In both cell types, deletion of the distal (−2832) and middle (−1477) fragments resulted in the highest level of luciferase activity, whereas constructs that contained all three domains showed minimal relative activity. A fragment bearing both proximal and middle domains displayed an intermediate level of activity (Figs. 2C and 2D).

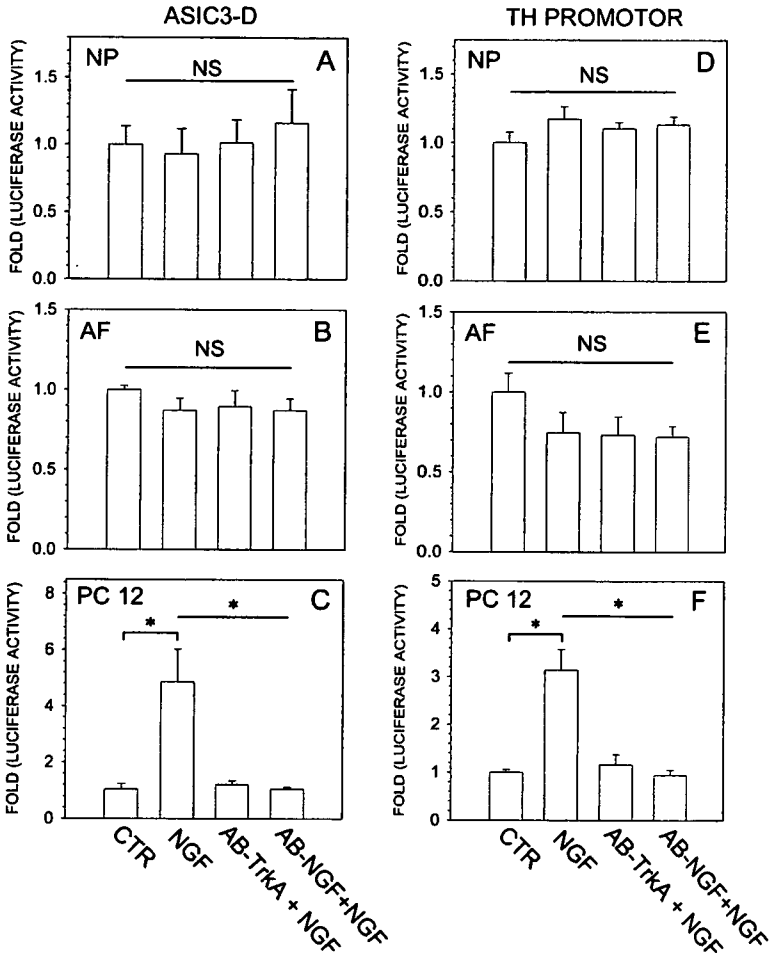

FIG. 3. Evaluation of ASIC3 promoter responsiveness to NGF treatment in nucleus pulposus, annulus fibrosus, and PC12 neuronal cells. Cells were transfected with full-length ASIC3 plasmid (ASIC3-D) and pRL-TK control vector and luciferase activity was measured 24 h after treatment with NGF (100 ng/ml). Note, in the nucleus pulposus (A) and annulus fibrosus cells (B), ASIC3 promoter activity did not change after NGF treatment, whereas in the PC12 cells (C), there was a 3- to 4-fold induction in promoter activity. NGF-mediated increase in ASIC3 promoter activity was suppressed to its basal level when PC12 cells were treated with anti-TrkA or anti-NGF antibody before addition of NGF. A similar experiment was performed using cells transfected with tyrosine hydroxylase (TH) promoter construct, a known NGF responsive gene. In both nucleus pulposus (D) and annulus fibrosus (E) cells, TH promoter activity did not change after NGF treatment. In contrast, in PC12 cells (F), a significant induction in activity was seen. The increase in TH promoter activity by NGF was suppressed by treatment with anti-TrkA or anti-NGF antibody. Values shown are mean ± SD of three independent experiments. $*p < 0.05$.

We evaluated the ASIC3 promoter activity of discal cells treated with NGF. Figure 3A shows that, when nucleus pulposus and annulus fibrosus cells were treated with rat NGF, ASIC3 promoter activity did not change. As a positive control, NGF responsive rat PC12 cells were used. These cells display a 4- to 5-fold increase in ASIC3 promoter activity after NGF treatment (Fig. 3C). Moreover, addition of anti-NGF or anti-TrkA antibody, before treatment with NGF, completely inhibited NGF-mediated induction of ASIC3 promoter activity. To further examine NGF responsiveness, we measured the promoter activity of tyrosine hydroxylase, a known NGF responsive gene. Figure 3 shows that, in both nucleus pulposus (Fig. 3D) and annulus fibrosus cells (Fig. 3E), NGF treatment did not upregulate tyrosine hydroxylase promoter activity. In contrast, in PC12 cells, there was a 3-fold induction in promoter activity; this response was completely inhibited by prior treatment with anti-NGF or anti-TrkA antibody (Fig. 3F).

We examined the expression of TrkA, a high-affinity NGF receptor, and p75NTR, a low-affinity NGF receptor, in untreated controls and in cells treated with NGF. Western blot analysis showed that nucleus pulposus cells have almost undetectable levels of TrkA protein under basal and stimulated conditions (Fig. 4A). However, there was a high expression of p75NTR under both conditions (Fig. 4A). Flow cytometric analysis confirmed that there was high expression of p75NTR (Fig. 4B). Because TrkA expression is low, we transfected nucleus pulposus with a full-length rat TrkA expression plasmid (Fig. 4C). Whereas Western blot analysis showed that transfected cells expressed high levels of TrkA protein and there was evidence of receptor phosphorylation, there was no substantive alteration in the level of p75NTR expression in nucleus pulposus cells.[22]

To learn if p75NTR was involved in maintenance of basal ASIC3 promoter activity in untreated nucleus pulposus cells, we suppressed its function using a function blocking anti-p75NTR antibody. Figure 5A shows that the anti-p75NTR antibody suppressed ASIC3 promoter activity by almost 40%. In a parallel experiment, nucleus pulposus cells were co-transfected with plasmid encoding ecdysone-inducible dominant negative form of p75NTR (DN-p75NTR), an ecdysone receptor plasmid pVgRxR and ASIC3 luciferase reporter. When treated with pronesterin-A (synthetic analog of ecdysone) to initiate expression of DN-p75NTR, there was a 40% decrease in ASIC3 basal promoter activity (Fig. 5B).

Because ERK is one of the key downstream effectors of p75NTR, we evaluated the role of this signaling molecule in

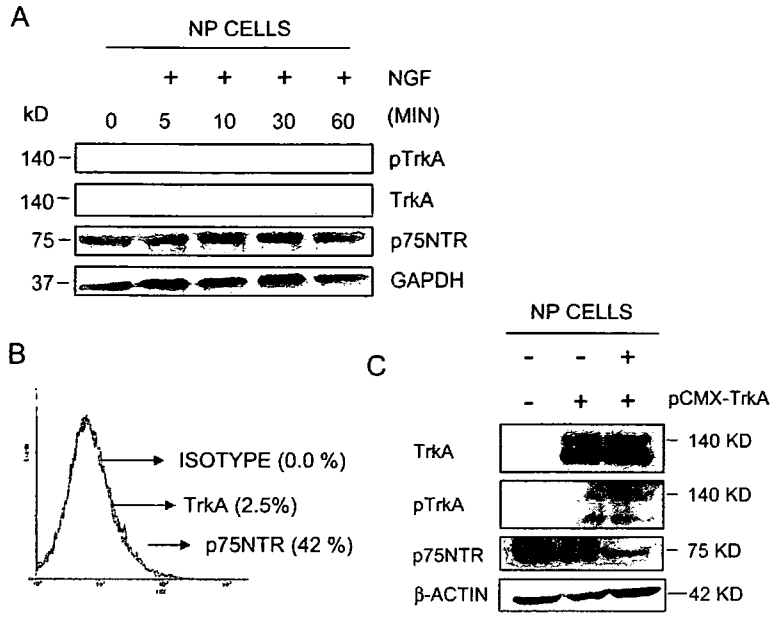

FIG. 4. Expression of TrkA and p75NTR in rat nucleus pulposus cells. (A) pTrkA and p75NTR expression in nucleus pulposus cells treated with NGF. Nucleus pulposus cells were treated with NGF (100 ng/ml), and TrkA and p75NTR expression and TrkA phosphorylation were analyzed by Western blot analysis over a 60-min time period. TrkA expression in nucleus pulposus cells was very low, and there was no indication of TrkA phosphorylation after NGF treatment. In contrast, nucleus pulposus cells showed robust expression of p75NTR. (B) Flow cytometric analysis of TrkA and p75NTR expression in nucleus pulposus cells. Cells were treated with anti-TrkA or p75NTR antibodies, and expression was analyzed by flow cytometry. Expression of TrkA in nucleus pulposus cells was very low or undetectable, whereas a high percentage of cells expressed p75NTR. (C) Effect of NGF on p75NTR and TrkA expression. Nucleus pulposus cells were transfected with rat TrkA expression plasmid, pCMX-TrkA, or did not receive any plasmid. Whole cell lysates were prepared, resolved on acrylamide gel, blotted, and probed with antibodies against TrkA, pTrkA, and β-actin. Nontransfected cells did not show detectable expression of TrkA or evidence of phosphorylation, whereas cells transfected with pCMX-TrkA expression plasmid robustly expressed TrkA and showed phosphorylated TrkA. There was a slightly higher level of TrkA phsophorylation in cells treated with NGF (100 ng/ml) after transfection with the pCMX-TrkA plasmid.

the maintenance of basal ASIC3 promoter activity in nucleus pulposus cells. Figure 6A shows that, after NGF treatment, there was a rapid increase in pERK1/2 levels. Expression was maximum at 5 min and declined rapidly thereafter, returning to basal levels by 3 h. To confirm that NGF-dependent transient activation of ERK signaling was mediated through p75NTR, we measured ELK1 transactivation (TAD function) in the presence of the DN-p75NTR plasmid. Figure 6B shows that NGF treatment significantly increased the activity of ELK-1; this activity was suppressed when DN-p75NTR expression was activated by pronesterin. We used a gain or loss of function approach to ascertain whether ERK was needed for maintenance of ASIC3 basal activity. When nucleus pulposus cells were cotransfected with the DN-MEK expression plasmid (Fig. 6C), there was a dose-dependent suppression in ASIC3 promoter activity. Inhibition of the ASIC3 reporter was evident even when the DN-MEK plasmid concentration was reduced to 50 ng. Furthermore, when cells were cotransfected with constitutively active (CA)-MEK1 expression plasmid, a dose-dependent increase in ASIC3 promoter activity was observed. At a CA-MEK plasmid dose of 50 ng, there was a 50% increase in ASIC3 promoter activity (Fig. 6D).

To explore the functional role of ASIC proteins, nucleus pulposus cells were treated with amiloride. A profound decrease in cell viability was observed in both hypertonic medium (Fig. 7A) and acidic culture conditions (Fig. 7B). To ascertain whether death was mediated by apoptosis, caspase-3 activity was measured in cells treated with amiloride under hypertonic conditions. Inhibition of ASIC function caused a significant increase in the fluorescence of the caspase-3 substrate PhiPhiLux G1D2, indicating that inhibition of the ASIC function promoted apoptosis (Figs. 7C and 7D). To further determine whether ASIC expression was mediated through the ERK pathway, nucleus pulposus cells were treated with the inhibitor PD98059 under hypertonic conditions. Figure 7E shows that, when cells are treated with the ERK inhibitor, there is dose-dependent loss of cell viability compared with amiloride treatment alone.

DISCUSSION

The experiments described in this study indicated that cells of the nucleus pulposus and inner annulus fibrosus contained ASIC channel proteins. This observation was surprising because the disc cells are notochordal in origin, and in the healthy state do not contain either sensory or motor neurons. We found that there was expression of ASIC3 and ASIC2b transcripts in both nucleus pulposus and annulus fibrosus tissue. Moreover, immunohistochemi-

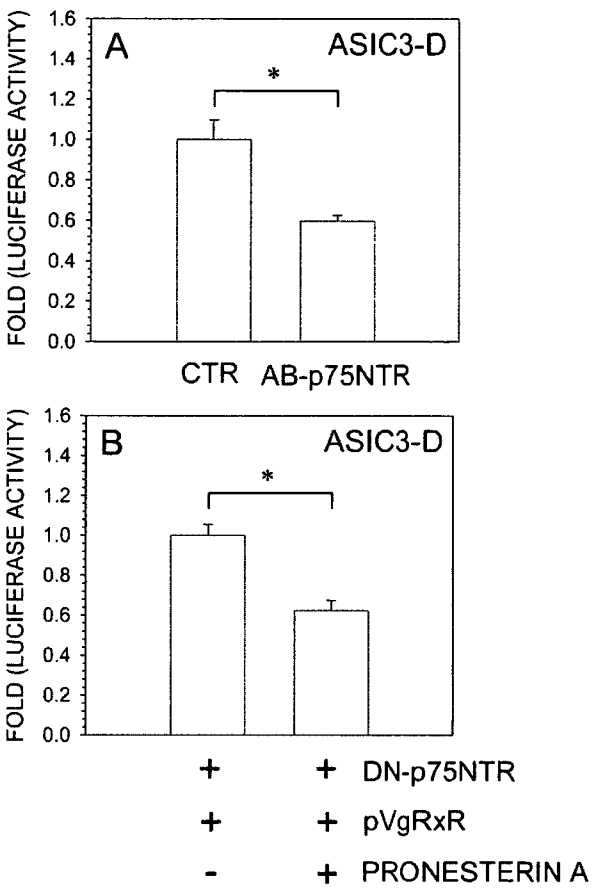

FIG. 5. Regulation of ASIC3 basal promoter activity by p75NTR in nucleus pulposus cells. (A) Effect of blocking p75NTR expression on ASIC3 promoter activity. Cells transfected with ASIC3-D plasmid were treated with anti-p75NTR antibody or isotype antibody (Ctr), and luciferase activity was measured 24 h after the treatment. When p75NTR function was blocked, there was a significant suppression in ASIC3 basal promoter activity. (B) Effect of expression of DN-p75NTR on ASIC3 promoter activity. Nucleus pulposus cells were co-transfected with ecdysone-inducible DN-p75NTR and ecdysone receptor pVgRxR plasmids along with ASIC3-D reporter. The cells were treated with 1 μg pronesterin-A for 24 h, and reporter activity was measured. Pronesterin-A–induced expression of DN-p75NTR resulted in ~50% suppression of ASIC3 promoter activity. Data shown are mean ± SD of three independent experiments performed in triplicate ($n = 3$). *$p < 0.05$.

cal and Western blot analysis revealed that there was expression of ASIC3 protein in nucleus pulposus cells of both the embryonic and adult rat discs; the protein was also expressed by cells of the inner annulus fibrosus. The presence of these ASIC isoforms in disc tissue lends strength to an earlier report that these proteins are functional components of connective tissues including both bone and cartilage.[23] It would not be unreasonable to assume that the functional activity of these channel proteins is linked to the glycolytic status of these tissues. In the disc, the limited vascularity would be expected to result in an accumulation of glycolytic byproducts, which would lower the discal pH and also increase the osmolarity of the extracellular matrix. pH-dependent Na^+ flux through the ASIC channel would serve to elevate the cation concentration and thereby promote restoration of the osmotic status of the tissue. From this perspective, rather than primarily serving a neurosensory function in the disc, the ASIC proteins function as "osmosensors" concerned with cell survival in a hydrodynamically stressed microenvironmental niche.

We evaluated the cellular localization of ASIC proteins using immunoblot and immunostaining assays. We noted a strong expression of both ASIC3 and ASIC2b proteins by the cultured disc cells. Western blot analysis of ASIC3 in rat nucleus pulposus cells indicated the existence of two bands: one at 60 kDa and one at 90 kDa. The 60-kDa band corresponded to the ASIC3 gene product reported in osteoblasts[23] or the 59 kDa, in vitro translated, nonglycosylated human ASIC3 protein.[9] With respect to the higher molecular weight protein (90 kDa), Alvarez de la Rosa et al.[24] and Leonard et al.[25] have reported an ASIC3 product with a molecular weight of 70–90 kDa. Our studies performed with the deglycosidase PNGase F indicated that the 90-kDa protein band does not represent an overglycosylated form of ASIC3. Whether the different molecular weight products is caused by alternate slicing or represents a separate gene product has not been determined. To learn if ASIC3 formed a heteromeric channel with ASIC2b, we performed immunoprecipitation assays, and in each case, evaluated the pulled down proteins. It was clear from this study that the ASIC proteins formed heteromeric channels in nucleus pulposus cells. In a parallel study, we observed expression of both ASIC proteins in the nuclear envelope. The possible functional importance of this latter finding is not known, but based on their physiological role in neural tissue, we cannot rule out the possibility that the channels maintain the charge balance between the nucleoplasm and cytoplasm in a pH-dependent manner.

Whereas details of the neuronal importance of the ASIC3 proteins are limited, Mamet et al.[17,26] have reported that, in rat dorsal root ganglion, the ASIC3 promoter is responsive to NGF through activation of the TrkA receptor. To ascertain if a similar regulatory system exists in disc cells, we examined ASIC3 promoter activity by transfection assays. In agreement with previous reports, the proximal domain construct exhibited maximal activity in both cell types,[26] whereas the full-length (2.8 kb) promoter with all three domains showed minimal activity. However, unlike neuronal cells, full-length promoter activity was not induced by NGF treatment of nucleus pulposus cells. Similarly, the tyrosine hydroxylase promoter, a known NGF-responsive gene promoter, did not respond to NGF treatment. In contrast to the nucleus pulposus, when PC12 cells were treated with NGF, there was a significant induction in both promoter activities.[18] This observation raised the following question: do cells of the nucleus pulposus possess functioning NGF receptors? To address this issue, we evaluated disc cells for the expression of high-affinity TrkA and low-affinity p75NTR receptors. These studies revealed that the p75NTR receptor was present in the nucleus pulposus cells.

Because the nucleus pulposus cells were refractory to NGF treatment, but showed expression of p75NTR, we ex-

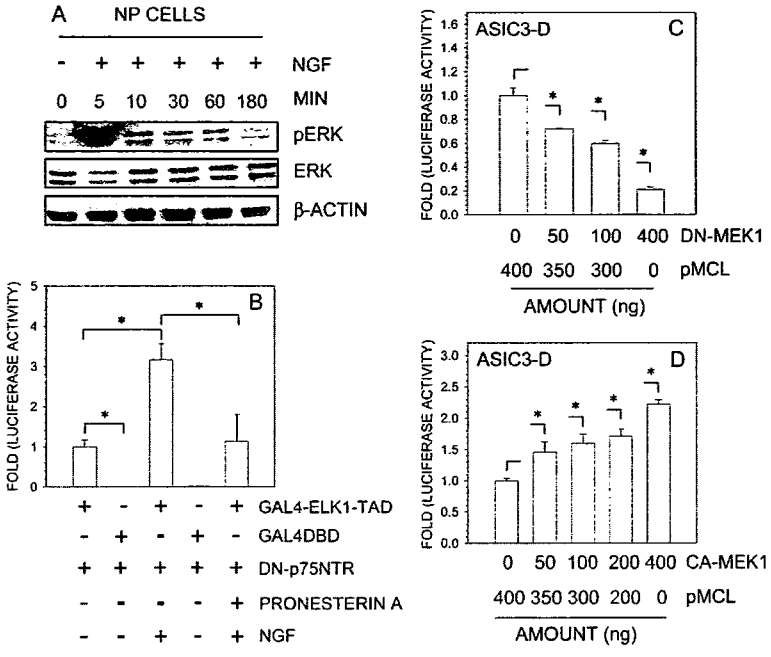

FIG. 6. Regulation of ASIC3 gene promoter by MEK/ERK signaling. (A) Influence of NGF treatment on ERK activity in nucleus pulposus cells. Cells were treated with NGF (100 ng/ml) for increasing time periods (0–180 min), and cell lysates were analyzed by Western blot. NGF treatment induced pERK1/2 expression within 5 min, and levels remained higher than basal levels for 1 h, although there was a decline after 10 min of exposure. (B) p75NTR-mediated activation of ERK in response to NGF treatment. Cells were co-transfected with ELK1-TAD plasmid (50 ng) or empty backbone vector (Gal4DBD; 50 ng) along with DN-p75NTR, and ELK1 transactivation was measured. NGF treatment significantly increased ELK1-TAD activity; the increase in activity was suppressed by pronesterin A–inducible DN-p75NTR. Backbone vector Gal4DBD showed minimal activity in untreated control cells and cells treated with NGF. (C) Effect of ERK inhibition on ASIC3 promoter activity. Cells were co-transfected with ASIC3-D reporter plasmid along with DN-MEK1 or empty backbone vector (pMCL), and reporter activity was measured. There was ~30% suppression of basal ASIC3 promoter activity with 50 ng DN-MEK plasmid, which was further suppressed at 100 ng. Further increases in DN-MEK plasmid concentration (up to 400 ng) suppressed basal reporter activity by almost 80%. (C) Effect of overexpression of MEK1 on ASIC3 promoter activity. Cells were co-transfected with CA-MEK1 expression vector or empty vector pMCL along with ASIC3-D reporter, and luciferase activity was measured. A significant induction in ASIC3 promoter activity was observed with 50 ng of MEK1 plasmid. When the dose of MEK1 plasmid was 400 ng, there was a 2.25-fold increase in ASIC3 reporter activity. Values shown are representative of three independent experiments, performed in triplicate; mean ± SD. $*p < 0.05$.

plored the possibility that this receptor was needed for ASIC3 expression. Using both a function blocking antibody and forced expression of the ecdysone inducible DN-p75NTR, we observed significant suppression in ASIC3 basal promoter activity. Although suppression was incomplete, indicating involvement of other factors in the regulation of basal ASIC3 promoter activity, these observations provide a basis for considering that the intervertebral disc cells possess a functionally active NGF-p75NTR signaling system that serves to regulate *ASIC3* gene expression. In support of this notion, it has recently been observed that intervertebral disc cells express functionally active NGF protein[27]; moreover, in an immunohistochemical study of cartilage tissue, Gigante et al.[28] reported the presence of NGF and p75NTR. Based on these findings, it is concluded that NGF binding to p75NTR, in autocrine or paracrine fashion, may serve to maintain basal ASIC3 expression in the discal tissues.

We explored the downstream regulation of ASIC3 activity in nucleus pulposus cells. One clue to the mechanism of transduction was the previous observation that all members of the neurotrophin family including NGF stimulate p75NTR-mediated rapid activation of ERK1/2[29]; this stimulation also occurs in cells that do not express TrkA. Our data confirmed that nucleus pulposus cells respond to NGF treatment by rapidly activating ERK1/2 and that this activation was mediated through p75NTR. To ascertain if p75NTR-mediated ERK signaling regulated the basal expression of ASIC3 promoter, both loss and gain of function approaches were used. As expected, forced expression of CA-MEK resulted in a dose-dependent induction of ASIC3 reporter activity. Co-transfection with DN-MEK, significantly suppressed basal ASIC3 promoter activity in a dose-dependent manner. In this case, because suppression was incomplete, there is the possibility that there is involvement of other signaling components. Based on these findings, it was concluded that MEK/ERK signaling is needed to maintain the basal promoter activity of ASIC3 in nucleus pulposus cells. Noteworthy, our previous studies have shown that the activities of this signaling pathway are responsible for maintenance of nucleus pulposus cell survival in hypoxic and hypertonic environments.[30,31]

Finally, it should be noted that, in nonskeletal tissues, one important consequence of reduced Na^+/H^+ exchange

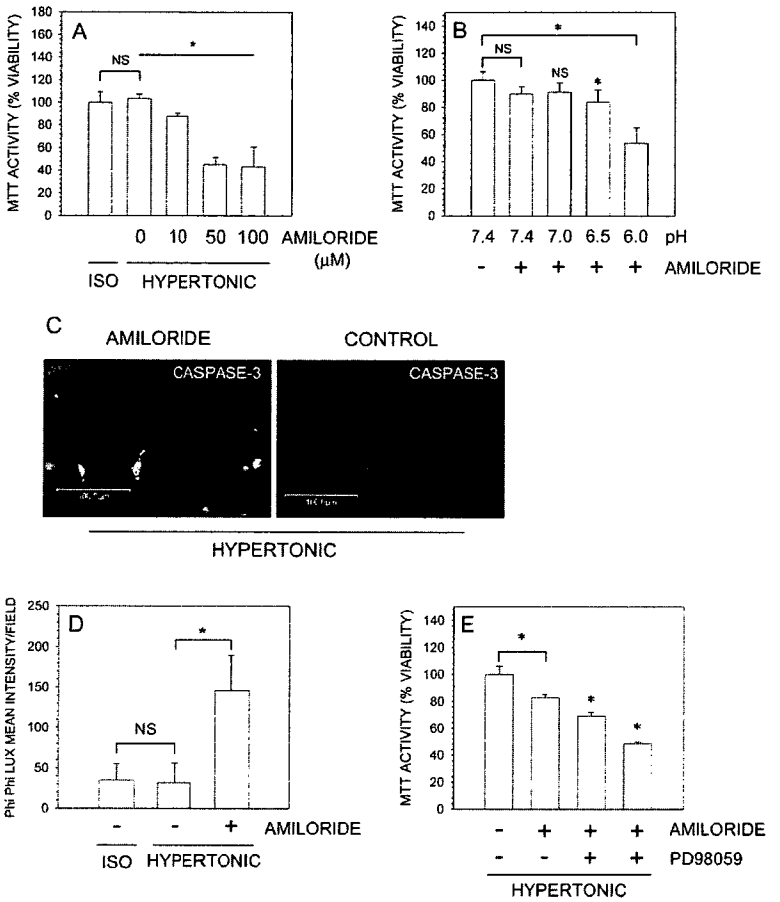

FIG. 7. Protective role of ASIC proteins in nucleus pulposus cells maintained in hypertonic and low pH media. (A) Survival of rat nucleus pulposus cells treated with with the ASIC inhibitor, amiloride, in hypertonic medium. Cells were treated with increasing concentrations of amiloride in hypertonic media for 24 h, and viability was measured by the MTT assay. An increase in tonicity from 330 (isotonic) to 450 mosmol/kg had no effect on nucleus pulposus cell viability. When cells were treated with amiloride (10–100 μM), a significant decrease in viability was observed. (B) Survival of rat nucleus pulposus cells treated with the ASIC inhibitor, amiloride, at different pH. Cells were treated with amiloride (10 μM) in different pH media for 24 h, and cell viability was measured by the MTT assay. Treatment with amiloride at pH 6.5 and 6.0 resulted in decreased cell viability. No change in viability was observed at pH 7.4 and 7.0. (C) Caspase-3 activity of nucleus pulposus cells in hypertonic medium. To assess the mode of cell death in hypertonic medium, nucleus pulposus cells were treated with amiloride (50 μM) for 24 h, incubated with the caspase-3 substrate PhiPhi Lux- G_1D_2, and evaluated by confocal microscopy. Note, a high number of amiloride-treated cells exhibit green fluorescence, showing increased activation of caspase-3, a proapoptotic molecule (magnification, ×20). (D) Quantitative image analysis of caspase-3 activity in nucleus pulposus cells maintained in hypertonic medium. Cells were treated as described above (C) and treated with PhiPhi Lux-G_1D_2. The fluorescence yield of cells maintained in isotonic and hypertonic media was comparable., Treatment with amiloride significantly increased the fluorescence yield, indicating increased caspase-3 activation leading to accelerated cell death by apoptosis, $*p < 0.05$. (E) Importance of the ERK pathway in mediating the ASIC response to hypertonicity. Nucleus pulposus cells were treated for 24 h with PD98059 (5 and 25 μM), along with amiloride (10 μM) in hypertonic medium. Simultaneous use of PD98059 and amiloride caused an increase in cell death compared with ASIC suppression alone. MTT values represent the mean ± SD of three independent experiments performed in triplicate. $*p < 0.05$.

activity is intracellular acidification, leading to compromised survival and sensitization to apoptosis.[32,33] In the disc, suppression of ASIC activity resulted in decreased nucleus pulposus cell survival and activation of the pro-apoptotic enzyme, caspase-3, in hyperosmotic and acidic media. Thus, aside from its evident role in pH homeostasis, ASIC3 seems to play a key role in protecting cells of the nucleus pulposus from hypertonic stress. From this perspective, ASIC3 and ASIC2b expression may permit adaptation of nucleus pulpous cells to their unique hydrodynamically stressed, hypoxic microenvironmental niche.

ACKNOWLEDGMENTS

This work was supported by a grant from the National Institutes of Health (AR050087).

REFERENCES

1. Hassler O 1969 The human intervertebral disc. A micro-angiographical study on its vascular supply at various ages. Acta Orthop Scand **40**:765–772.
2. Rajpurohit R, Risbud MV, Ducheyne P, Vresilovic EJ, Shapiro IM 2002 Phenotypic characteristics of the nucleus pulposus:

Expression of hypoxia inducing factor-1, glucose transporter-1 and MMP-2. Cell Tissue Res **308**:401–407.
3. Risbud MV, Guttapalli A, Stokes DG, Hawkins D, Danielson KG, Schaer TP, Albert TJ, Shapiro IM 2006 Nucleus pulposus cells express HIF-1alpha under normoxic culture conditions: A metabolic adaptation to the intervertebral disc microenvironment. J Cell Biochem **98**:152–159.
4. Grunder S, Geissler HS, Bassler EL, Ruppersberg JP 2000 A new member of acid-sensing ion channels from pituitary gland. Neuroreport **11**:1607–1611.
5. Garcia-Anoveros J, Derfler B, Neville-Golden J, Hyman BT, Corey DP 1997 BNaC1 and BNaC2 constitute a new family of human neuronal sodium channels related to degenerins and epithelial sodium channels. Proc Natl Acad Sci USA **94**:1459–1464.
6. Lingueglia E, de Weille JR, Bassilana F, Heurteaux C, Sakai H, Waldmann R, Lazdunski M 1997 A modulatory subunit of acid sensing ion channels in brain and dorsal root ganglion cells. J Biol Chem **272**:29778–29783.
7. Chen CC, England S, Akopian AN, Wood JN 1998 A sensory neuron-specific, proton-gated ion channel. Proc Natl Acad Sci USA **95**:10240–10245.
8. Waldmann R, Champigny G, Bassilana F, Heurteaux C, Lazdunski M 1997 A proton-gated cation channel involved in acid-sensing. Nature **386**:173–177.
9. Bassilana F, Champigny G, Waldmann R, de Weille JR, Heurteaux C, Lazdunski M 1997 The acid-sensitive ionic channel subunit ASIC and the mammalian degenerin MDEG form a heteromultimeric H+-gated Na+ channel with novel properties. J Biol Chem **272**:28819–28822.
10. Reeh PW, Kress M 2001 Molecular physiology of proton transduction in nociceptors. Curr Opin Pharmacol **1**:45–51.
11. Hesselager M, Timmermann DB, Ahring PK 2004 pH Dependency and desensitization kinetics of heterologously expressed combinations of acid-sensing ion channel subunits. J Biol Chem **279**:11006–11015.
12. Sutherland SP, Benson CJ, Adelman JP, McCleskey EW 2001 Acid-sensing ion channel 3 matches the acid gated current in cardiac ischemia-sensing neurons. Proc Natl Acad Sci USA **98**:711–716.
13. Sluka KA, Price MP, Breese NM, Stucky CL, Wemmie JA, Welsh MJ 2003 Chronic hyperalgesia induced by repeated acid injections in muscle is abolished by the loss of ASIC3, but not ASIC1. Pain **106**:229–239.
14. Sluka KA, Radhakrishnan R, Benson CJ, Eshcol JO, Price MP, Babinski K, Audette KM, Yeomans DC, Wilson SP 2007 ASIC3 in muscle mediates mechanical, but not heat, hyperalgesia associated with muscle inflammation. Pain **129**:102–112.
15. Yagi J, Wenk HN, Naves LA, McCleskey EW 2006 Sustained currents through ASIC3 ion channels at the modest pH changes that occur during myocardial ischemia. Circ Res **99**:501–509.
16. Jones RC III, Xu L, Gebhart GF 2005 The mechanosensitivity of mouse colon afferent fibers and their sensitization by inflammatory mediators require transient receptor potential vanilloid 1 and acid-sensing ion channel 3. J Neurosci **25**:10981–10989.
17. Mamet J, Baron A, Lazdunski M, Voilley N 2002 Proinflammatory mediators, stimulators of sensory neuron excitability via the expression of acid-sensing ion channels. J Neurosci **22**:10662–10670.
18. Suzuki T, Kurahashi H, Ichinose H 2004 Ras/MEK pathway is required for NGF-induced expression of tyrosine hydroxylase gene. Biochem Biophys Res Commun **315**:389–396.
19. Meakin SO, Gryz EA, MacDonald JI 1997 A kinase insert isoform of rat TrkA supports nerve growth factor-dependent cell survival but not neurite outgrowth. J Neurochem **69**:954–967.
20. Vaidya RJ, Ray RM, Johnson LR 2005 MEK1 restores migration of polyamine-depleted cells by retention and activation of Rac1 in the cytoplasm. Am J Physiol Cell Physiol **288**:C350–C359.
21. Khwaja F, Allen J, Lynch J, Andrews P, Djakiew D 2004 Ibuprofen inhibits survival of bladder cancer cells by induced expression of the p75NTR tumor suppressor protein. Cancer Res **64**:6207–6213.
22. Rankin SL, Guy CS, Mearow KM 2005 TrkA NGF receptor plays a role in the modulation of p75NTR expression. Neurosci Lett **383**:305–310.
23. Jahr H, van Driel M, van Osch GJ, Weinans H, van Leeuwen JP 2005 Identification of acid-sensing ion channels in bone. Biochem Biophys Res Commun **337**:349–354.
24. Alvarez de la Rosa D, Zhang P, Shao D, White F, Canessa CM 2002 Functional implications of the localization and activity of acid-sensitive channels in rat peripheral nervous system. Proc Natl Acad Sci USA **99**:2326–2331.
25. Leonard AS, Yermolaieva O, Hruska-Hageman A, Askwith CC, Price MP, Wemmie JA, Welsh MJ 2003 cAMP-dependent protein kinase phosphorylation of the acid-sensing ion channel-1 regulates its binding to the protein interacting with C-kinase-1. Proc Natl Acad Sci USA **100**:2029–2034.
26. Mamet J, Lazdunski M, Voilley N 2003 How nerve growth factor drives physiological and inflammatory expressions of acid-sensing ion channel 3 in sensory neurons. J Biol Chem **278**:48907–48913.
27. Abe Y, Akeda K, An HS, Aoki Y, Pichika R, Muehleman C, Kimura T, Masuda K 2007 Proinflammatory cytokines stimulate the expression of nerve growth factor by human intervertebral disc cells. Spine **32**:635–642.
28. Gigante A, Bevilacqua C, Pagnotta A, Manzotti S, Toesca A, Greco F 2003 Expression of NGF, Trka and p75 in human cartilage. Eur J Histochem **47**:339–344.
29. Lad SP, Neet KE 2003 Activation of the mitogen-activated protein kinase pathway through p75NTR: A common mechanism for the neurotrophin family. J Neurosci Res **73**:614–626.
30. Risbud MV, Fertala J, Vresilovic EJ, Albert TJ, Shapiro IM 2005 Nucleus pulposus cells upregulate PI3K/Akt and MEK/ERK signaling pathways under hypoxic conditions and resist apoptosis induced by serum withdrawal. Spine **30**:882–889.
31. Risbud MV, Di Martino A, Guttapalli A, Seghatoleslami R, Denaro V, Vaccaro AR, Albert TJ, Shapiro IM 2006 Toward an optimum system for intervertebral disc organ culture: TGF-beta 3 enhances nucleus pulposus and annulus fibrosus survival and function through modulation of TGF-beta-R expression and ERK signaling. Spine **31**:884–890.
32. Schneider D, Gerhardt E, Bock J, Muller MM, Wolburg H, Lang F, Schulz JB 2004 Intracellular acidification by inhibition of the Na+/H+-exchanger leads to caspase-independent death of cerebellar granule neurons resembling paraptosis. Cell Death Differ **11**:760–770.
33. Kim KM, Lee YJ 2005 Amiloride augments TRAIL-induced apoptotic death by inhibiting phosphorylation of kinases and phosphatases associated with the P13K-Akt pathway. Oncogene **24**:355–366.

Address reprint requests to:
Makarand V Risbud, PhD
Department of Orthopaedic Surgery
Thomas Jefferson University
1015 Walnut Street, Suite 501, Curtis Building
Philadelphia, PA 19107, USA
E-mail: makarand.risbud@jefferson.edu

Received in original form March 9, 2007; revised form June 26, 2007; accepted August 9, 2007.

Transplantation of Mesenchymal Stem Cells in a Canine Disc Degeneration Model

Akihiko Hiyama,[1,2] Joji Mochida,[1,2] Toru Iwashina,[1,2] Hiroko Omi,[1,2] Takuya Watanabe,[1,2] Kenji Serigano,[1,2] Futoshi Tamura,[1,2] Daisuke Sakai[1,2]

[1]Department of Orthopaedic Surgery, Surgical Science, Tokai University School of Medicine, Bohseidai, Isehara, Kanagawa, 259-1193, Japan

[2]Center for Regenerative Medicine, Tokai University School of Medicine, Bohseidai, Isehara, Kanagawa, 259-1193, Japan

Received 5 August 2007; accepted 18 October 2007

Published online in Wiley InterScience (www.interscience.wiley.com). DOI 10.1002/jor.20584

ABSTRACT: Transplantation of mesenchymal stem cells (MSCs) is effective in decelerating disc degeneration in small animals; much remains unknown about this new therapy in larger animals or humans. Fas-ligand (FasL), which is only found in tissues with isolated immune privilege, is expressed in IVDs, particularly in the nucleus pulposus (NP). Maintaining the FasL level is important for IVD function. This study evaluated whether MSC transplantation has an effect on the suppression of disc degeneration and preservation of immune privilege in a canine model of disc degeneration. Mature beagles were separated into a normal control group (NC), a MSC group, and the disc degeneration (nucleotomy-only) group. In the MSC group, 4 weeks after nucleotomy, MSCs were transplanted into the degeneration-induced discs. The animals were followed for 12 weeks after the initial operation. Subsequently, radiological, histological, biochemical, immunohistochemical, and RT-PCR analyses were performed. MSC transplantation effectively led to the regeneration of degenerated discs. FACS and RT-PCR analyses of MSCs before transplantation demonstrated that the MSCs expressed FasL at the genetic level, not at the protein level. GFP-positive MSCs detected in the NP region 8 weeks after transplantation expressed FasL protein. The results of this study suggest that MSC transplantation may contribute to the maintenance of IVD immune privilege by the differentiation of transplanted MSCs into cells expressing FasL. © 2008 Orthopaedic Research Society. Published by Wiley Periodicals, Inc. J Orthop Res

Keywords: mesenchymal stem cells; intervertebral disc; disc degeneration, nucleus pulposus; regenerative medicine

INTRODUCTION

It has been reported that 80% of the human population experiences low back pain at least once in their lifetime; the consequent pressure of medical costs and occupational injuries on the economy has been a major social problem.[1,2] Although most low back pain is believed to be caused by disc degeneration, for which various causes have been reported,[3,4] the details of the mechanism of disc degeneration have not yet been clearly identified. Histologically, a normal disc consists of a central nucleus pulposus (NP) surrounded by the annulus fibrosus (AF), and upper and lower endplates. The NP mainly consists of water and a proteoglycan (PG)-rich extracellular matrix with type II collagen fibers. In contrast, the AF is composed primarily of concentric collagen type I-rich annular lamella.[5,6] To treat disc disorders, fusion techniques have been widely used, but postoperative problems, such as instability of adjacent intervertebral discs (IVDs), often occur.[7,8] Therefore, motion preservation through the development of new treatments for the control of disc degeneration is desirable, and various biological strategies aimed at the repair and regeneration of degenerated discs have been suggested.[9–16]

Recently, in the field of regenerative medicine, mesenchymal stem cells (MSCs) have received widespread attention because, depending on their environment, they have multilineage potential (bone, cartilage, and fat), and in addition, they are immune tolerant.[17,18] MSCs are found in small numbers, about 0.125% of the cells, in the bone marrow stroma.[19] Although there are no specific markers for the phenotypes of NP and AF cells, they share cell characteristics similar to those of chondrocytes.[20] Because the chondrocytic

Correspondence to: D. Sakai (Telephone: 81-463-93-1121, ext. 2320; Fax: 81-463-96-4404;
E-mail: daisakai@is.icc.u-tokai.ac.jp)

phenotype can be induced in MSCs, it is believed that the chondrocyte-like cells among NP and AF cells may be derived from MSCs. Sakai et al.[21–23] reported that disc degeneration can be decelerated following MSC transplantation in a degenerative disc model, and that it may be possible to induce site-dependent differentiation of MSCs into NP cells. Crevensten et al.[24] demonstrated that MSCs injected into the rat disc, using a hyaluronan gel as a scaffold, maintained viability and proliferated. In that study, viable cells were detected, using cell labeling, over a 28-day period and the disc height was maintained.[24] Other research groups, who have conducted additional tests on MSC transplantation in a degenerative disc model, have reported the potential of cell-based transplantation therapy.[25,26] However, many factors involved in the transplantation of MSCs, such as the environment in the IVD after MSC transplantation and the induction of MSCs by NP cells, remain unknown. In addition, all the studies thus far have been done in small laboratory species whose NP cells differ from those of humans and larger animals. Therefore, to investigate the future usefulness of MSC transplantation in humans, it is essential to study its effects in larger animals.

IVDs, particularly the NP, are considered by their anatomical properties to be avascular tissues surrounded by a thick AF and endplates. Because of their isolation from the immune system of the host, IVDs are included among the tissues that have a so-called immune privilege. Tissues that have this type of immune privilege include the retina,[27] testes,[28] and brain.[29] It has been shown that FasL, a transmembrane protein of the tumor necrosis factor (TNF) family, plays an important role in maintaining immune privilege.[30] Cytotoxic T lymphocytes (CTLs) and natural killer (NK) cells show cytotoxic activity after being activated,[30] and are thought to cause apoptosis by stimulating the Fas of the target cells (transplanted cells or virus-infected cells), which act as foreign bodies to the host.[31] Protection from exposure to CTL or NK cells, in which cytotoxic substances (such as TNF-α or perforin) are released through the expression of FasL by target cells, constitutes an immune response reaction that exists in the immune-privileged tissues mentioned above, including the IVD. Takada et al.[32] have reported that FasL is expressed in normal IVDs as well. In a recent study, it was reported that the number of cells expressing FasL, which is involved in immune privilege, is reduced by disc degeneration; the molecular mechanism of FasL for controlling disc degeneration has been a recent focus of research. However, no studies have been conducted on the generation of FasL by IVD cells following MSC transplantation. When transplanted, MSCs act as foreign bodies to the host IVD cells. It is believed that the IVD cells, which have immune privilege, eliminate the MSCs via the Fas–FasL system. Along with immune tolerant nature of MSCs, it is unpredictable what will happen at the molecular level when MSCs are transplanted to the IVD. In this study, we investigated whether it was possible for MSC transplantation to limit the IVD degeneration induced by nucleotomy in a larger animal (the dog), as well as to examine how MSC transplantation affects immune privilege, including Fas–FasL, in the processes of degeneration and regeneration of discs.

MATERIALS AND METHODS

Animal experiments were carried out according to a protocol approved by the Animal Experimentation Committee at our institution. Mature beagle dogs (10–13 months old; $n = 18$; mean weight about 10 kg; Nosan Beagle, Nosan Corporation, Kanagawa, Japan) were separated into three groups: a normal control (NC) group, a group that received a MSC transplantation following nucleotomy to induce disc degeneration (MSC), and a disc degeneration-only group (nucleotomy only). Lateral radiographs and magnetic resonance imaging (MRI) were performed before the surgical treatment, and parameters, such as disc space narrowing and vertebral abnormalities, were determined. No vertebral or disc abnormalities were found in the animals used in this study.

Degenerative Disc Model

After the intramuscular administration of atropine sulfate (0.05 mg/kg, Tanabe Pharmacy, Inc., Osaka, Japan) and xylazine (2.0 mg/kg, ROMPUN, Bayer Health Care, Inc., Leverkusen, Germany), disc degeneration was induced under inhalation anesthesia with 2.5% isoflurane (Abbott Laboratories, North Chicago, IL). The discs to be punctured were carefully exposed at regions L3/4, L4/5, and L5/6. An 18-gauge needle was inserted at the center of the disc through the AF into the NP. To induce disc degeneration, the NP was aspirated using a 10-mL syringe, as previously described.[33,34] The mean weight of NP aspirated from a single disc was 16.6 ± 3.5 mg. None of the animals had problems related to the surgery, and all regained full function.

Bone Marrow Collection, Bone Marrow Analyses, and Transplantation of MSCs

During the initial surgery, MSCs were also harvested from the iliac crests. According to the method described previously,[22] the collected bone marrow was carefully separated and mononucleated cells were seeded into

 DOI 10.1002/jor

100-mm dishes with Dulbecco's modified Eagles medium (DMEM) supplemented with 10% fetal bovine serum (FBS) and antibiotics (100 U/mL penicillin, and 100 μg/mL streptomycin) at 37°C, 5% CO_2. After 2 days, the adherent cells were considered to be autologous MSCs. Every 48 h, the medium was changed and nonadherent cells were removed. To facilitate analysis of the survival of transplanted MSCs in the NP region, the MSCs were then infected with AcGFP1, a retrovirus vector expressing the green fluorescent protein (GFP) gene (conditioning studies were performed, data not shown). Vector incorporation was more than 90% (data not shown) using FACS analysis. Following the second passage in culture, the cells were cultured for 19.2 ± 4.1 days (12–27days), autologous MSCs were enzymatically released from monolayer culture. The recovered MSCs were stained with anti-FasL (sc-834, Santa Cruz Biotech, Santa Cruz, CA) and anti-keratan sulfate (KS) (MAB2022, Chemicon international, CA) antibodies, and analyzed for differences in cell size and internal composition using a FACS Vantage cell sorter prior to transplantation. We also extracted total RNA from the MSCs and used semiquantitative reverse-transcription polymerase chain reaction (RT-PCR) to determine FasL mRNA expression before transplantation. At 4 weeks after the first operation, 1×10^6 autologous MSCs were percutaneously transplanted into the IVDs in which degeneration had been induced (L3/4, L4/5, and L5/6) using a discogram needle (27-gauge) under fluoroscopic imaging. To assure that the cells were placed into an intact nucleus cavity and would not leak out through an annular fissure, the intradiscal pressure was determined before introducing the cells.[35]

Evaluations

Radiological Assessment

Lateral radiographs were taken under inhalation anesthesia in all groups before harvest at baseline (0 weeks) and at 4, 8, and 12 weeks following the first operation ($n = 18$). A fluoroscopic imaging intensifier (radiographs; 70 kV, 10 mA, distance 100 cm) was used. The radiography images were scanned and stored using digital photography, and all images were evaluated using image J software program (free online software, Image Processing and Analysis). The measurements included vertebral body height and IVD height. The analyzed data were transferred to the Excel software program (Microsoft, Excel 2003). The disc height index (DHI), using the method of Masuda et al.,[36] was calculated for comparisons between groups. The percent disc height index {%DHI = (postoperative DHI /preoperative DHI) × 100} was subsequently calculated and the %DHI at each experimental level was compared to that in the NC group.

MRI Assessment

MRIs were taken for evaluation of signal changes in T2-weighted images in all groups at each time point. After the intramuscular administration of atropine sulfate (0.05 mg/kg) and xylazine (2.0 mg/kg), MRIs were taken under inhalation anesthesia in all dogs ($n = 18$). The MRIs were performed using only a spine coil (Gyroscan, ACS-NT, Powertrak6000, Philips, Best, The Netherlands). T2-weighted sections in the sagittal plane were obtained using the following settings: fast spin echo sequence with time to repetition (TR) of 4000 ms and time to echo (TE) of 150 ms; interslice gap: 0.3 mm; matrix: 512 × 512; field of view (FOV): 200 × 200 mm; number of excitations: 4; TSE echo spacing: 18.8). The MRIs were classified using the Pfirrmann modification 12 weeks after the first operation.[37,38] Three observers, blinded to this study, performed the grading for each image; the average grade of the three observers was used as the final grade for each disc. The intraobserver reliability based on readings at two time intervals 1 month apart was $\kappa = 0.90$, showing an excellent agreement.

Macroscopic Findings

The final radiographs and MRIs were obtained, the dogs were euthanized with a lethal dose of sodium pentobarbital (120 mg/kg) (Abbott Laboratories), and the L3/4, L4/5, and L5/6 spinal segments were harvested together with their cranial and caudal vertebral bodies. The spinal segments from two dogs from each group of six dogs ($n = 6$ IVDs) were fixed in 10% formalin neutral buffer solution (Wako, Osaka, Japan) and decalcified in Plank-Rychlo solution (Decalcifying Solution A; Wako). Each specimen was cut longitudinally at the center of the disc for macroscopic evaluation.

Histological Examination

After macroscopic evaluation, specimen discs (L3/4, L4/5, and L5/6) were excised from the lumbar spine of different two dogs from each group and each IVD was fixed in 10% formalin, decalcified, embedded in paraffin, sectioned, and assessed by histology and immunostaining ($n = 6$ IVDs). These were stained with hematoxylin and eosin and Safranin-O for evaluation. Two observers blinded to this study and familiar with human and animal IVD specimens performed the evaluation of these sections. The intraobserver error was very small. The kappa value for grading scale was 0.88, showing an excellent agreement.

Biochemical Analyses

Specimen discs (L3/4, L4/5, and L5/6) were removed from lumbar spine of two dogs from each group ($n = 6$ IVDs). Using a dissecting microscope, the tissue from the NP region of each IVD in each group was detached from the upper and lower endplates with careful manipulation. These excised discs were then digested for 48 h at 55°C in a papain solution (200 μg/mL in 0.1 M Na acetate, 50 mmol/L EDTA, 5 mmol/L L-cysteine, at pH 5.53). The papain digests were analyzed to

determine the total sulfated glycosaminoglycan (GAG) content, as an indicator of total PG content, using the dimethylmethylene blue (DMMB) dye-binding method as previously described.[39] The total PG content of each sample was normalized by its total DNA content as measured by the bisbenzimidazole fluorescent dye method (Hoechst 33258).[40] The data were expressed as micrograms of PG per microgram of DNA and were compared among groups by calculating the percentage of the normal control, using the mean data of the NC group discs as the control value. All assays were performed in duplicate.

Immunohistochemical Staining for FasL and Fas

Immunohistochemistry was performed using formalin-fixed sections obtained from each group as described above. Immunohistochemical staining was used to evaluate the expression of FasL and Fas using the streptavidin–biotin method. Although the anti-FasL antibody used in this study was goat specific, it can be used in dogs because of adequate crossreactivity (data not shown). Briefly, after nonspecific binding was blocked by incubating with 10% normal goat serum for 1 h, the sections were labeled overnight at 4°C with anti-goat FasL and anti-Fas polyclonal antibodies (immunoglobulin G) (sc-834, and sc-715: 1:50 and 1:50; Santa Cruz Biotech, Santa Cruz, CA), prepared at an optimum dilution of 1:100 in PBS. Biotinylated antigoat IgG (VECTASTAIN, Vector laboratories, Inc., Burlingame, CA) and streptavidin were then added. After washing and removing excess buffer, the sections were covered with 3,3′-diaminobenzidine (DAB) substrate until a brown color developed. Finally, the sections were counterstained with hematoxylin. Two pathologists counted the total disc cells and FasL and Fas-positive disc cells within 10 high power fields (HPFs; magnification ×400) for each of three sections in each group. The percentage of FasL- and Fas-positive disc cells to total disc cells was calculated.

Immunocytochemical Triple Staining

Immunocytochemistry was performed on formalin-fixed sections from six discs that had received MSC transplantation. The sections were stained with an anti-GFP primary antibody (sc-5385: 1:50; Medical & Biological Laboratories, Nagoya, Japan) and an antigoat FasL polyclonal antibody immunoglobulin G (sc-834: 1:50; Santa Cruz Biotech). Alexa 488 and 594 (1:100; Molecular Probes, Invitrogen Corporation, Carlsbad, CA) were used as secondary antibodies, respectively, for anti-GFP and anti-goat FasL. Tissues on the slides were mounted with VECTASHIELD mounting medium with 4′,6′-diamino-2-phenylindole (DAPI) (Vector Laboratories).

Expression of FasL Genes by RT-PCR

The RT-PCR technique was used to determine FasL mRNA expression at 8 weeks after the MSC transplantation. Specimen discs (L3/4, L4/5, and L5/6) were removed from the spines of two dogs from each group and individually processed for RT-PCR ($n = 6$ IVDs). Total RNA was isolated after harvest by mincing the discs using a sterile scalpel. The pieces were then snap-frozen and pulverized in liquid nitrogen and the tissue powder was homogenized with Isogen reagent (Nippon-gene, Tokyo, Japan) and then further purified using RNeasy spin columns (Qiagen, Valencia, CA). Absorbances at 260 and 280 nm were measured for RNA quantification and quality control. RNA samples were then reverse transcribed to cDNA using oligo dT primer and Multiscribe Reverse Transcriptase followed by the SV Total RNA Isolation System (Promega corporation, Madison, WI). PCR amplification was carried out using a two-step protocol of a 10-min pre-PCR heat step at 95°C for activation of AmpliTaq Cold DNA polymerase (Applied Biosystems, Tokyo, Japan), followed by 40 cycles of denaturing at 95°C for 15 s and annealing at 60°C for 1 min. The PCR products were separated electrophoretically using nondenaturing 1.2% TBE polyacrylamide gels and stained with ethidium bromide. The upstream and downstream primer sequences for each primer are as follows: FasL (XM_848916:5′-caagatccatccctctggaa-3′ 5′-gcttgttgttgcaggactga-3′ β-actin (Z70044:5′-ggcatcctgaccctgaagta-3′ 5′-acgtacatggttggggtgtt-3′. The primers were designed using the Primer3 software program (MIT, free download at http://www-genome.wi.mit.edu/cgi-bin/primer/primer3_www.cgi) using sequence data from the National Center for Biotechnology Information GenBank database. The gels were scanned under UV light with a Densitograph system (Atto Biotechnologies Inc, Tokyo, Japan), and band intensities were semiquantified densitometrically and normalized to β-actin gene values using a CS Analyzer (Version, 2.01, Atto corporation, Tokyo, Japan).

Statistical Analyses

The significance of differences among means of data on radiograph measurements, biochemical parameters, the total score of the histological grading, and the RT-PCR analyses were analyzed by two-way repeated measures analysis of variance (ANOVA), or one-way ANOVA and the Fisher's PLSD post hoc test. The Kruskal-Wallis test and Mann-Whitney *U*-test were used to analyze nonparametric data (MRI and histology grading for each parameter). The Statview program was used for the statistical analyses. Significance was accepted at $p < 0.05$. Error bars were set to represent the standard deviation (SD).

RESULTS

Results of Radiographic and MRI Analyses

Disc height, presented as %DHI that was measured and calculated from plain radiographs, is shown in Figure 1A. At 4, 8, and 12 weeks after the first

DOI 10.1002/jor

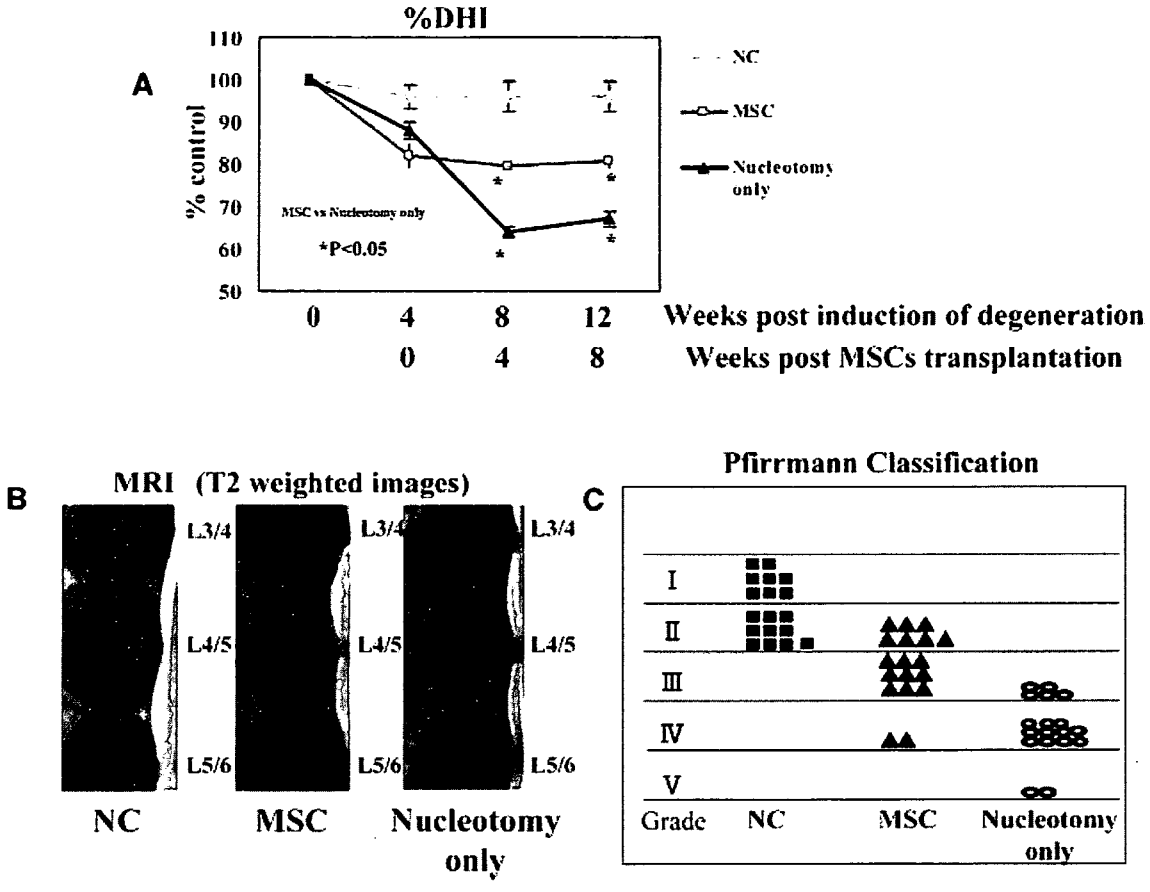

Figure 1. Radiographic and MRI analyses. (A) No significant decrease in %DHI occurred at any time point in the NC group. At 8 and 12 weeks, the MSC-transplantation group exhibited a significant delay in the progression of disc degeneration compared to the nucleotomy-only group (*$p < 0.05$, the Fisher's PLSD post hoc test). (B) At 12 weeks after the first operation, representative MRI (T2 images) of the nucleus pulposus (NP) in the MSC-transplanted group showed stronger signal intensities than those in the nucleotomy-only group. (C) Analysis of signal changes in T2-weighted images at 12 weeks after the first operation using the Phirrmann classification, based on changes in the degree and area of signal intensity from grades 1 to 5. A significantly lower grading of MRI in the MSC-transplanted group (2.72 ± 0.70) compared to the nucleotomy-only group (3.83 ± 0.62) was found ($p = 0.0039$, $p < 0.01$ Mann-Whitney test).

operation, the %DHI in both the MSC-transplanted group and the disc degeneration group (nucleotomy only) was significantly decreased compared to the NC group (NC: 4w, $96.1 \pm 2.9\%$; 8w, $96.0 \pm 3.6\%$; 12w, $96.0 \pm 3.6\%$. MSC: 4w, $82.0 \pm 2.9\%$; 8w, $79.7 \pm 0.5\%$, 12w, $80.6 \pm 1.4\%$. Nucleotomy only: 4w, $87.9 \pm 2.0\%$; 8w, $68.1 \pm 3.0\%$, 12w, $67.0 \pm 1.9\%$) (Fig. 1A). At 8 and 12 weeks postinduction of disc degeneration, the variation in %DHI between the MSC-transplanted group and the nucleotomy-only group was statistically significant ($p < 0.05$. $p = 0.0019$ and $p = 0.0005$, respectively).

At 12 weeks after the first operation, the MRI (T2 images) of the NP in the MSC-transplanted group showed stronger signal intensities than those in the nucleotomy-only group (Fig. 1B). In the nucleotomy-only group, the NP area signal intensity, as a percentage of preoperative values, continued to decrease (data not shown). In contrast, the MSC-transplanted group demonstrated a significant increase in the NP area signal intensity (data not shown). The MRI grading points, using the Pfirrmann classification (from grades 1 to 5), confirmed a significant ($p < 0.05$) delay in the progression of disc degeneration in the MSC-transplanted group at 12 weeks after the first operation. At 4 weeks after the induction of disc degeneration and before the transplantation of MSCs, for the MSC-transplanted group, the Pfirrmann grade mean value was 2.89 ± 0.67. There were no significant differences in the other two groups. Comparing the MRI grading of the

degree of disc degeneration at 12 weeks after the first operation between the MSC-transplanted group (2.72 ± 0.70) and the nucleotomy group (3.83 ± 0.62), a significantly lower grading of MRI in the MSC-transplanted group was found ($p = 0.0039, p < 0.01$ Mann-Whitney test). The MRI grading of the degree of disc degeneration in the MSC-transplanted group (2.72 ± 0.70) was significantly higher when compared to the NC group (1.56 ± 0.51) ($p = 0.0018$, $p < 0.01$ Mann-Whitney test) (Fig. 1C).

Results of Macroscopic Findings

Based on macroscopic evaluations, in the MSC-transplanted group the discs showed a structure similar to those in the NC group, whereas the discs from the nucleotomy-only group showed disc space narrowing and connective tissue invasion (Fig. 2).

Results of Histlogical Analyses

The histological analyses also demonstrated noteworthy regenerative effects from MSC transplantation. Normal-looking discs in the NC group displayed an intact AF with a normal pattern of fibrocartilage lamellas and a well-defined border between the NP and AF (Fig. 3A). The MSC-transplanted group discs showed a relatively well preserved inner annulus structure compared to discs from the nucleotomy-only group (Fig. 3B). Safranin-O staining results revealed an increased staining in the MSC-transplanted group, while a remarkable decrease in staining could be seen in the nucleotomy-only group (Fig. 3C).

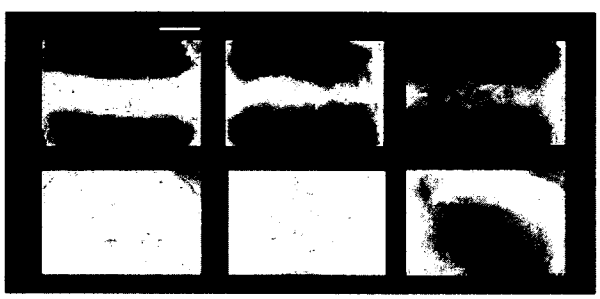

Figure 2. Macroscopic views of intervertebral discs at 12 weeks after induction of disc degeneration by nucleotomy. In the MSC group, 4 weeks after nucleotomy, autologous MSCs were transplanted into the degenerated intervertebral discs (IVDs). A representative disc of the MSC-transplanted group shows an oval-shaped gel-like nucleus pulposus (NP) similar to that of a representative disc from the NC group. A disc representative of the nucleotomy-only group shows narrowing of disc height and changes in the NP structure. Bar = 5 mm.

Results of Biochemical Analyses

The biochemical analysis showed that the PG content of the MSC-transplanted group (5.92 ± 0.25 μg PG/μg DNA) was similar to that of the NC group (6.17 ± 0.49 μg PG/μg DNA), whereas the PG content of the nucleotomy-only group (5.44 ± 0.17 μg PG/μg DNA) showed a significant decrease, compared to the NC group ($p < 0.001$). The PG contents of the IVDs of the MSC-transplanted group were significantly increased over those of the nucleotomy-only group ($p < 0.001$, two-way ANOVA). When the PG content was expressed as a percentage of the averaged data for the NC group ($n = 6$ IVDs), the MSC-transplant group was $95.8 \pm 3.9\%$ and the nucleotomy group was $88.2 \pm 2.7\%$. There is a significant difference between NC group and nucleotomy group) ($p < 0.01$, two-way ANOVA).

Results of Immunohistochemical Staining and Analysis of Fas Ligand (FasL) and Fas

Immunohistochemical staining for FasL in canine IVDs showed that the proportion of FasL-positive cells increased following MSC-transplantation at 12 weeks after the first operation, compared to nucleotomy only, to approximate the level found in the NC group (Fig. 4B). The proportion of FasL-positive cells in the nucleotomy-only group was significantly decreased from that of the MSC-transplanted group (NC: $27.7 \pm 11.1\%$; MSC: $29.0 \pm 14.1\%$; nucleotomy only: $18.4 \pm 13.5\%$, $p < 0.05$) (Fig. 4B). Compared to the NC group, the proportion of Fas-positive cells in the NP region increased after induction of disc degeneration in the nucleotomy group, but that proportion was suppressed after MSC-transplantation (NC: $20.2 \pm 13.8\%$; MSC: $28.0 \pm 10.9\%$; nucleotomy only: $34.6 \pm 18.9\%$, $p < 0.05$) (Fig. 4C).

Results of mRNA Expression of KS and FasL and Cell Survival of MSCs and Immunohistochemical Triple-Staining Analyses

Based on FACS analysis, before transplantation, the expression of KS was detected in about 30–40% of the MSCs; however, FasL was not expressed (Fig. 5A). We also found FasL mRNA expression in MSCs to be at a very low level when compared to KS mRNA expression (Fig. 5B). This result suggests that, before transplantation, FasL may be expressed in the MSCs at the gene level but not at the protein level. We did find that some of the GFP-positive MSCs in the NP region costained with FasL upon immunocytochemical triple staining after transplantation (Fig. 5C). The

DOI 10.1002/jor